



ELSEVIER

Contents lists available at SciVerse ScienceDirect

Applied Mathematical Modelling

journal homepage: www.elsevier.com/locate/apm

Analysis of microwave induced natural convection in a single mode cavity (Influence of sample volume, placement, and microwave power level)

W. Klinbun^a, P. Rattanadecho^{b,*}

^a Rattanakosin College for Sustainable Energy and Environment (RCSEE), Rajamangala University of Technology Rattanakosin, Puthamonthon Sai 5, Salaya, Nakornpathom 73170, Thailand

^b Research Center of Microwave Utilization in Engineering (RCME), Department of Mechanical Engineering, Thammasat University (Rangsit Campus), Klong Luang, Pathumthani 12120, Thailand

ARTICLE INFO

Article history:

Received 23 November 2009
 Received in revised form 30 May 2011
 Accepted 1 July 2011
 Available online 22 July 2011

Keywords:

Microwave heating
 Rectangular waveguide
 Mode TE₁₀
 Maxwell's equation
 FDTD method

ABSTRACT

The heating of water layer using microwave oven with a rectangular waveguide has been studied both numerically and experimentally. The mathematical model is validated with the experimental data. The transient Maxwell's equations are solved by using the Finite Difference Time Domain (FDTD) method to describe the electromagnetic field inside the waveguide and sample. The temperature profile and velocity field within sample are determined by the solutions of the momentum, energy and Maxwell's equations. In this study, the effects of physical parameters, e.g. microwave power level, placement of sample inside the waveguide, volume of sample, are studied. The distribution of electric field, temperature profile and velocity field are presented in details. The results show good agreement between simulation results and experimental data. Conclusively, the mathematical model presented here correctly explains the phenomena of microwave heating of water layer.

© 2011 Elsevier Inc. All rights reserved.

1. Introduction

Microwave is a new heat source and more attractive than the conventional heating methods because an electromagnetic wave can penetrate through the surface and is converted into thermal energy within the materials. This results in increase very rapid temperature. In addition, microwave technology has several advantages, such as high speed startup, selective energy absorption; instantaneous electric control, energy efficiency and non pollution. Thus, microwave energy is used in many industrial processes and household oven. The successful examples of microwave application include food drying, pasteurization, sterilization, vulcanization processing, curing of concrete, medical sterilization and process adhesives.

In the past microwave power absorbed was assumed to decay exponentially into the sample following the Lambert's law. For example, Datta et al. [1] predicted the volumetric heat source by using Lambert's law and analyzed the temperature profile in liquid. However, this assumption is valid for the large dimension samples where the depth of sample is larger than the penetration depth but for the thin samples, the depth of sample is smaller than penetration depth, heat transfer rate by microwave is faster. Therefore, the spatial variations of the electromagnetic field within thin samples must be obtained by solution of the Maxwell's equations.

The models interactions between the electromagnetic field and the dielectric materials have been used previously to study numerous heating processes of the dielectric materials in a variety of microwave applicators such as a rectangular waveguide and the cavities. Jia and Bialkowski [2], Liu et al. [3], Dibben and Metaxas [4] determined the electromagnetic field inside microwave application by using Maxwell's equations. The electromagnetic field inside a waveguide filled

* Corresponding author. Tel.: +662 564 3001x3153; fax: +662 564 3010.
 E-mail address: ratphadu@engr.tu.ac.th (P. Rattanadecho).

Nomenclature

C_p	specific heat capacity (J/(kg K))
E	electric field intensity (V/m)
f	frequency of incident wave (Hz)
g	gravitational constant (m/s^2)
H	magnetic field intensity (A/m)
P	power (W)
p	pressure (Pa)
Q	local electromagnetic heat generation term (W/m^3)
s	Poynting vector (W/m^2)
T	temperature ($^{\circ}C$)
t	time (s)
$\tan \delta$	loss tangent coefficient (-)
u, w	velocity component (m/s)
Z_H	wave impedance (Ω)
Z_I	intrinsic impedance (Ω)

Greek letters

α	thermal diffusivity (m^2/s)
β	coefficient of thermal expansion (1/K)
η	absolute viscosity (Pa s)
ϵ	electrical permittivity (F/m)
λ	wavelength (m)
μ	magnetic permeability (H/m)
v	velocity of propagation (m/s)
ν	kinematics viscosity (m^2/s)
ρ	density (kg/m^3)
σ	electric conductivity (S/m)
ω	angular frequency (rad/s)
ζ	surface tension (N/m)

Subscripts

∞	ambient condition
r	relative
a	air
in	input
w	water

partially with a dielectric material was investigated by Tada et al. [5]. The results showed the correlations between the power absorption ratio and the position of the dielectric in the guide and permittivity of the dielectric. The sharp maximum happened when the dielectric is located around the middle of the applicator. Zhang et al. [6] purposed three dimensional distribution of microwave inside a cavity by solving Maxwell's equations with Finite Difference Time Domain technique and to obtain temperature profile and flow field within liquid sample (distilled water and corn oil) by using finite control volume based on SIMPLER algorithm.

The previous studies investigated the effects of physical parameters by using mathematical modeling on understanding the complex physics that arose during microwave heating of liquids. Ayappa et al. [7], they studied numerically the natural convection of liquid in a square cavity that exposed to traveling plane microwave. They found the location, intensity, and number of power peaks had affected on uniformity of temperature distribution in liquid. Chatterjee et al. [8] investigated numerically the heating of containerized liquid using microwave radiation. The effects of turntable rotation, natural convection, power source and aspect ratio of container on the temperature profile were studied and they presented detailed results of temperature profiles, stream functions and time evolution of flow filed. Results indicated turntable rotation did not aid in achieving uniform heating in case of a symmetric heat source. Zhu et al. [9] presented numerical model to study heat transfer in liquids that flowed continuously in a circular duct that was subjected to microwave heating. The results showed the heating pattern strongly depends on the dielectric properties of the fluid in the duct and the geometry of microwave heating system.

Although analysis of microwave heating in liquids layer are more increase than the past, the few papers investigate the fluid motion that arise during microwave heating of liquids with a full comparison between mathematical modeling and experimental data. This is because of complex distribution of electromagnetic wave in cavity that is a complicated effect on flow field. Rattanadecho et al. [10] investigated microwave heating of liquid sample in a rectangular waveguide by numerically and experimentally. Microwave was operated in TE_{10} mode at a frequency of 2.45 GHz. The movement of liquid

induced by microwave energy was taken into account. Coupled electromagnetic, flow field and thermal profile were simulated in two dimensional. Their work showed the effects of liquid electric conductivity and microwave power level on the degree of penetration and rate of heat generation within liquid layer. Results showed that the heating kinetic strongly depends on the dielectric properties.

In addition, there are many papers in this field such as Basak [11], Ratanadecho et al. [12,13], Rattanadecho et al. [14], Cham et al. [15,16] and Klinbun et al. [17]. This work will extend from the work of Ratanadecho et al., [10]. The objectives are to investigate the effects of microwave power level, placement of liquid layer inside the waveguide, and volume of liquid layer on distributions of electric field inside a rectangular waveguide, temperature profile and flow pattern within a liquid layer.

2. Experiment setup

The experiment apparatus is showed in Fig. 1. The microwave system is a monochromatic wave of TE_{10} mode with operating frequency of 2.45 GHz. Microwave is generated by magnetron and is transmitted along the Z-direction of a rectangular waveguide with inside dimensions of $109.2 \text{ mm} \times 54.6 \text{ mm}$ toward a water load that is situated at the end of the waveguide. On the upstream side of the sample, an isolator is used to trap any microwave reflected from the sample to prevent the microwave from damaging the magnetron. The powers of incident, reflected and transmitted waves are measured by a wattmeter using a directional coupler (MICRO DENSHI., model DR-5000). Fiber optic (LUXTRON Fluoroptic Thermometer., model 790, accurate to $\pm 0.5 \text{ }^\circ\text{C}$) is employed for temperature measurement. The fiber optic probes are inserted into the sample, and situated on the XZ plane at $Y = 25 \text{ mm}$. Due to the symmetrical condition, temperatures are measured for only one side of the plane. An initial temperature of sample is $28 \text{ }^\circ\text{C}$ for all cases. A sample container with a thickness of 0.75 mm is made from polypropylene which does not absorb microwaves.

3. Mathematical modeling

The schematic diagram of the problem is showed in Fig. 2. The water contained in container is filled inside the guide. The side and bottom walls of container are insulated except the upper surface is opened. The water in case of full load means cross section area ($X \times Z$) are $109.2 \times 54.6 \text{ mm}^2$ while cross section area in case of partial load are $54.6 \times 54.6 \text{ mm}^2$. The coordinate system designated by XYZ is used to describe electromagnetic fields and the system, xyz, is designated for describing temperature and flow fields.

3.1. Analysis of electromagnetic field inside a rectangular waveguide

Microwave field in the TE_{10} mode does not have variation of field in the direction between the broad faces of the rectangular waveguide; this means that the microwave is uniform in the Y-direction. Consequently, it is assumed two dimensional flow and heat transfer model in X and Z directions would be sufficient to identify the microwave heating phenomena in a rectangular waveguide. The water layer is assumed to be homogeneous and isotropic. The other assumptions are as follows:

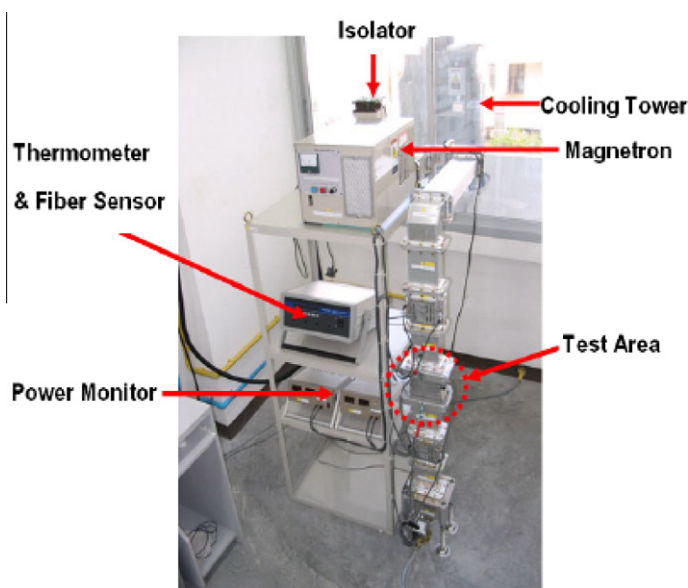


Fig. 1. Experimental apparatus of microwave heating in TE_{10} mode.

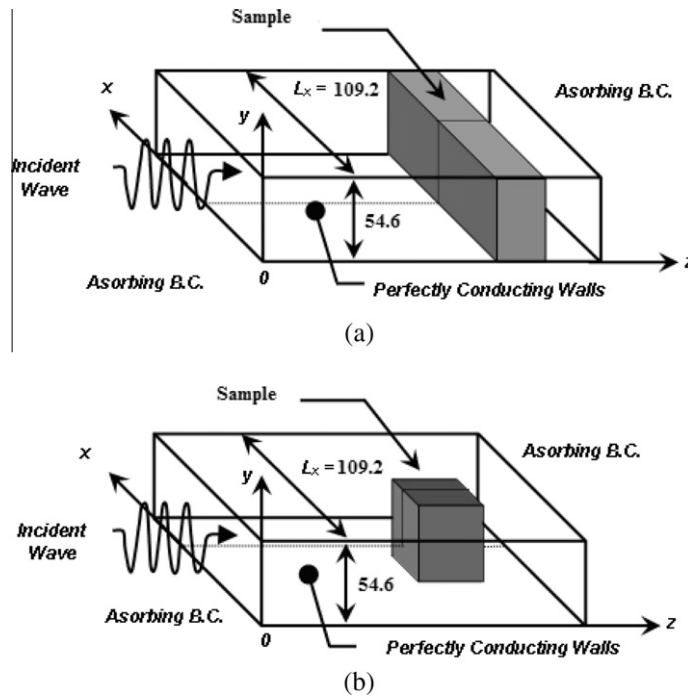


Fig. 2. Schematic diagram of the problem: (a) full load case; (b) partial load case.

- (1) The absorption of microwave by air inside a rectangular waveguide is negligible.
- (2) The walls of rectangular waveguide are perfect electric conductors.
- (3) The effect of sample container on the electromagnetic and temperature field can be neglected.

Maxwell's equations governing the electromagnetic field are expressed in terms of the electric field, E , and the magnetic field, H . In the Cartesian coordinate system (X, Y, Z) , they are given in TE₁₀ mode as:

$$E_x = E_z = H_y = 0, \quad (1)$$

$$\frac{\partial E_y}{\partial t} = \frac{1}{\varepsilon} \left(\frac{\partial H_x}{\partial Z} - \frac{\partial H_z}{\partial X} - \sigma E_y \right), \quad (2)$$

$$\frac{\partial H_z}{\partial t} = -\frac{1}{\mu} \frac{\partial E_y}{\partial X}, \quad (3)$$

$$\frac{\partial H_x}{\partial t} = \frac{1}{\mu} \frac{\partial E_y}{\partial Z}, \quad (4)$$

where $\varepsilon = \varepsilon_0 \varepsilon_r$ is the electrical permittivity, σ is the electrical conductivity and $\mu = \mu_0 \mu_r$ is the magnetic permeability. In this study, the dielectric properties depend only on temperature, as follows:

$$\varepsilon_r(T) = \varepsilon_r'(T) - j\varepsilon_r''(T), \quad (5)$$

where ε_r' is the relative dielectric constant of the liquid, characterizes the penetration of microwave energy into the product, while, the relative dielectric loss factor, ε_r'' , indicates the ability of the product to convert the microwave energy into heat [9]. The loss tangent coefficient, $\tan \delta$, can be expressed as follows:

$$\tan \delta = \frac{\varepsilon_r''}{\varepsilon_r'}, \quad (6)$$

$\tan \delta$ indicates the ability of the product to absorb microwave energy.

When the material is heated unilaterally, it is found that as the dielectric constant and loss tangent coefficient vary, the penetration depth will be changed and the electric field within the dielectric material is altered. The penetration depth is used to denote the depth at which the power density has decreased to 37% of its initial value at the surface [10].

$$D_p = \frac{1}{\frac{2\pi f}{v} \sqrt{\frac{\epsilon_r' \left(\sqrt{1 + \left(\frac{\epsilon_r''}{\epsilon_r'}\right)^2} - 1 \right)}{2}}} = \frac{1}{\frac{2\pi f}{v} \sqrt{\frac{\epsilon_r' (\sqrt{1 + (\tan \delta)^2} - 1)}{2}}}, \tag{7}$$

where D_p is penetration depth, ϵ_r'' is relative dielectric loss factor. And v is microwave speed. The penetration depth of the microwave power is calculated according to Eq. (7), which shows how it depends on the dielectric properties of the material. It is noted that products with huge dimensions and high loss factors, may occasionally overheat on the outer layer. To prevent such phenomenon, the power density must be chosen so that enough time is provided for the essential heat exchange between boundary and core. If the thickness of the material is less than the penetration depth, only a fraction of the supplied energy will become absorbed. In example, consider the dielectric properties of water typically show moderate lossiness depending on the temperature. The water layer at low temperature typically shows slightly greater potential for absorbing microwaves. In the other word, an increasing in the temperature typically decreases ϵ_r'' , accompanied by a slight increment in D_p .

The boundary conditions for analysis of electromagnetic field can be formulated as follows:

- (1) At the walls of waveguide are assumed to be perfect conducting wall and are given by Faraday's law and Gauss's theorem:

$$E_t = 0, \quad H_n = 0, \tag{8}$$

where t, n denote tangential and normal component, respectively.

- (2) Along the interface between sample and air are given by Ampere's law and Gauss's theorem:

$$\begin{aligned} E_t &= E_t', & H_t &= H_t', \\ D_n &= D_n', & B_n &= B_n'. \end{aligned} \tag{9}$$

- (3) At both ends of the rectangular waveguide, the Mur's first order absorbing conditions [20] are applied:

$$\frac{\partial E_Y}{\partial t} = \pm v \frac{\partial E_Y}{\partial Z}. \tag{10}$$

where v is phase velocity of wave propagation.

- (4) Oscillation of the electric and magnetic intensities by magnetron. For incident waves due to magnetron are given by [10]:

$$E_Y = E_{Yin} \sin\left(\frac{\pi X}{L_X}\right) \sin(2\pi ft), \tag{11}$$

$$H_X = \frac{E_{Yin}}{Z_H} \sin\left(\frac{\pi X}{L_X}\right) \sin(2\pi ft), \tag{12}$$

where E_{Yin} is the input value of electric field intensity, L_X is the length of the rectangular waveguide in the X-direction, Z_H is the wave impedance defined as

$$Z_H = \frac{\lambda_g Z_l}{\lambda} = \frac{\lambda_g}{\lambda} \sqrt{\frac{\mu}{\epsilon}}. \tag{13}$$

Here Z_l is intrinsic impedance depending on the properties of the material, λ and λ_g are the wavelength of microwaves in free space and rectangular waveguide, respectively.

The power flux associated with a propagating electromagnetic wave is expressed by the Poynting vector:

$$s = \frac{1}{2} \text{Re}(E \times H^*). \tag{14}$$

Table 1
The electromagnetic and thermo physical properties used in the computations [10].

$\epsilon_0 = 8.85419 \times 10^{-12}$ [F/m]	$\mu_0 = 4.0\pi \times 10^{-7}$ [H/m]
$\epsilon_{ra} = 1.0$	$\mu_{rw} = 1.0$
$\mu_{ra} = 1.0$	
$\tan \delta_a = 0.0$	
$\rho_a = 1.205$ [kg/m ³]	$\rho_w = 1000$ [kg/m ³]
$C_{pa} = 1.007$ [kJ/(kg K)]	$C_{pw} = 4.186$ [kJ/(kg K)]
$\lambda_a = 0.0262$ [W/(m K)]	$\lambda_w = 0.610$ [W/(m K)]

The Poynting theorem allows the evaluation of the microwave power input. It is represented as

$$P_{in} = \int_A S dA = \frac{A}{4Z_H} E_{in}^2. \quad (15)$$

3.2. Analysis of flow and heat transfer within water layer

To reduce complexity of the problem, several assumptions have been offered into the momentum and energy equations.

- (1) Corresponding to analysis of electromagnetic field, considering flow and temperature field can be assumed to be two-dimensional plane.
- (2) The effect of the phase change of the water layer can be neglected.
- (3) The water layer is assumed by the Boussinesq approximation.
- (4) The side and bottom walls of the water layer are insulated except the upper wall can exchange with the ambient air.

Continuity equation

$$\frac{\partial u}{\partial x} + \frac{\partial w}{\partial z} = 0. \quad (16)$$

Momentum equation

$$\frac{\partial u}{\partial t} + u \frac{\partial u}{\partial x} + w \frac{\partial u}{\partial z} = -\frac{1}{\rho} \frac{\partial p}{\partial x} + \nu \left(\frac{\partial^2 u}{\partial x^2} + \frac{\partial^2 u}{\partial z^2} \right), \quad (17)$$

$$\frac{\partial w}{\partial t} + u \frac{\partial w}{\partial x} + w \frac{\partial w}{\partial z} = -\frac{1}{\rho} \frac{\partial p}{\partial z} + \nu \left(\frac{\partial^2 w}{\partial x^2} + \frac{\partial^2 w}{\partial z^2} \right) + g\beta(T - T_\infty), \quad (18)$$

where ν and β are the kinematics viscosity and coefficient of thermal expansion of the water layer, respectively.

Energy equation

$$\frac{\partial T}{\partial t} + u \frac{\partial T}{\partial x} + w \frac{\partial T}{\partial z} = \alpha \left(\frac{\partial^2 T}{\partial x^2} + \frac{\partial^2 T}{\partial z^2} \right) + Q, \quad (19)$$

where Q is the local electromagnetic heat generation term in W/m^3 , that is a function of the electric field and defined as

$$Q = 2\pi f \epsilon_0 \epsilon_r' \tan \delta (E_Y)^2. \quad (20)$$

Boundary and initial conditions for Eqs. (16)–(19):

Since the walls of container are rigid, the velocities are zero. At the interface between liquid layer and the walls of container, zero slip boundary conditions are used for the momentum equations.

- (1) At the upper surface, the velocity in normal direction (w) and shear stress in the horizontal direction are assumed to be zero, where the influence of Marangoni flow [10] can be applied:

$$\eta \frac{\partial u}{\partial z} = -\frac{d\xi}{dT} \frac{\partial T}{\partial x}, \quad (21)$$

where η and ξ are the absolute viscosity and surface tension of liquid layer, respectively.

- (2) The side and bottom walls, except the top wall, are insulated so no heat and mass exchanges:

$$\frac{\partial T}{\partial x} = \frac{\partial T}{\partial z} = 0. \quad (22)$$

- (3) Heat is lost from the upper surface via natural convection:

$$\lambda \frac{\partial T}{\partial z} = h_c (T - T_\infty), \quad (23)$$

where h_c is the local heat transfer coefficient.

The initial condition of a water layer is defined as:

$$T = T_0 \quad \text{at } t = 0. \quad (24)$$

4. Numerical solution

The description of heat transport and flow pattern of water layer equations (16)–(19) requires specification of temperature (T), velocity component (u, w) and pressure (p). These equations are coupled to the Maxwell's equations (Eqs. (2)–(4)) by Eq. (20). It represents the heating effect of the microwaves in the liquid-container domain.

4.1. Electromagnetic equations and FDTD discretization

The electromagnetic equations are solved by using Finite Difference Time Domain (FDTD) method. With this method the electric field components (E) are stored halfway between the basic nodes while magnetic field components (H) are stored at the center. So they are calculated at alternating half-time steps. E and H field components are discretized by a central difference method (second-order accurate) in both spatial and time domain. For TE mode, the electric and magnetic field components are discretized as:

$$E_y^n(i, k) = \frac{1 - \frac{\sigma(i,k)\Delta t}{2\epsilon(i,k)}}{1 + \frac{\sigma(i,k)\Delta t}{2\epsilon(i,k)}} E_y^{n-1}(i, k) + \frac{\Delta t}{\epsilon(i, k)} \frac{1}{1 + \frac{\sigma(i,k)}{2\epsilon(i,k)}} \left\{ \frac{H_z^{n-1/2}(i + 1/2, k) - H_z^{n-1/2}(i - 1/2, k)}{\Delta x} + \frac{H_x^{n-1/2}(i, k - 1/2) - H_x^{n-1/2}(i, k + 1/2)}{\Delta z} \right\}, \tag{25}$$

$$H_x^{n+1/2}(i, k + 1/2) = H_x^{n-1/2}(i, k + 1/2) + \frac{\Delta t}{\mu(i, k + 1/2)} \left\{ \frac{E_y^n(i, k + 1) - E_y^n(i, k)}{\Delta z} \right\}, \tag{26}$$

$$H_z^{n+1/2}(i + 1/2, k) = H_z^{n-1/2}(i + 1/2, k) - \frac{\Delta t}{\mu(i + 1/2, k)} \left\{ \frac{E_y^n(i + 1, k) - E_y^n(i, k)}{\Delta x} \right\}. \tag{27}$$

4.2. Fluid flow and heat transport equations and finite control volume discretization

Eqs. (16)–(19) are solved numerically by using the finite control volume (FCV) along with the SIMPLE algorithm developed by Patankar [18]. The reason to use this method is the advantages of flux conservation that avoids generation of parasitic source. The basic strategy of the finite control volume discretization method is to divide the calculated domain into a number of control volumes and then integrate the conservation equations over this control volume over an interval of time $[t, t + \Delta t]$. At the boundaries of the calculated domain, the conservation equations are discretized by integrating over half the control volume and taking into account the boundary conditions. At the corners of the calculated domain we used a quarter of control volume. The fully implicit time discretization finite difference scheme is used to arrive at the solution in time. Additionally, the details about numerical discretization of this method can be found in the recent literature.

4.3. The stability and accuracy of calculation

The choice of spatial and temporal resolution is motivated by reasons of stability and accuracy. Spatially, as shown in Fig. 3, Eqs. (25)–(27) are solved on a grid system, and temporally they are solved alternatively for both the electric and magnetic fields. To ensure stability of the time stepping algorithm Δt must be chosen to satisfy the Courant stability condition and defined as

$$\Delta t \leq \frac{\sqrt{(\Delta x)^2 + (\Delta z)^2}}{v}. \tag{28}$$

And the spatial resolution of each cell, defined as

$$\Delta x, \Delta z \leq \frac{\lambda_g}{10\sqrt{\epsilon_r}}. \tag{29}$$

Corresponding to Eqs. (28) and (29), the calculation conditions are as follows:

- (1) Grid size: $\Delta x = 1.0922$ mm and $\Delta z = 1.0000$ mm.
- (2) Time steps: $\Delta t = 2 \times 10^{-12}$ s and $\Delta t = 0.01$ s are used corresponding to electromagnetic field and temperature field calculations, respectively.
- (3) Number of grids: $N = 100$ (width) $\times 160$ (length).
- (4) Relative error in the iteration procedures of 10^{-6} was chosen.

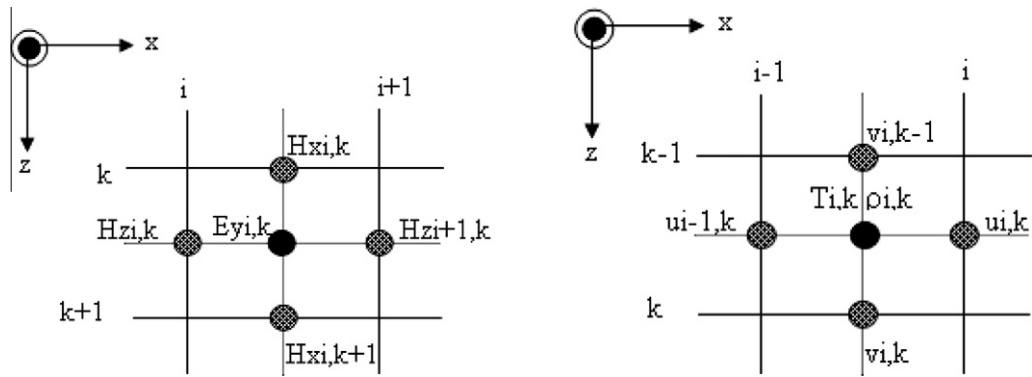


Fig. 3. Grid system configuration [19].

4.4. The iterative computational schemes

Since the dielectric properties of liquid layer samples are temperature dependent, to understand the influence of electromagnetic field on microwave heating of liquid layer realistically it is necessary to consider the coupling between electric field and temperature and fluid flow fields. For this reason, the iterative computational schemes are required to resolve the coupled non-linear Maxwell's equations, momentum and heat transport equations.

The computational scheme is to first compute a local heat generation term by running an electromagnetic calculation with uniform properties determined from initial temperature data. The electromagnetic calculation is performed until a sufficient period is reached in which representative average rms (root mean square) of the electric field at each point is computed and used to solve the time dependent temperature and velocities field. Using these temperatures new values of the dielectric properties are calculated and use to re-calculate the electromagnetic fields and then the microwave power absorption. All the steps are repeated until the required heating time is reached. The detail of computational schemes and strategy are illustrated in Fig. 4.

5. Results and discussion

The results are divided into four parts. Part I is model validation, mathematical simulations of microwave heating in water layer were compared with experimental results. Part II to VI are showed the effects of microwave power level, placement of water layer inside the waveguide, and volume of water layer, respectively (see Table 1).

5.1. Mathematical model validation

Figs. 5 and 6 show the comparison of the temperature distribution within the water layer between the simulation results and experimental data at various times, along with the horizontal axis ($z = 10$ mm) and vertical axis ($x = 54.6$ mm) of a rectangular waveguide, respectively. Which correspond to those of initial temperature with 28 °C and microwave power level of 300 W. Fig. 5 shows the greatest temperature in the center of heating layer with the temperature decreasing towards the side walls of the water layer corresponding to the characteristic of TE_{10} mode. However, the results from calculation at the side walls are increasing again. It is because of the walls are insulated so rate of heat loss must be low. Fig. 6, the temperature within the water layer closest to the incoming microwave is shown. The region close to the top surface heats up with a faster rate than elsewhere within the water layer. Nevertheless, the temperature decays slowly along the propagation direction due to the skin depth heating effect. All in all, the predicted results are in a reasonable agreement with the experimental results.

5.2. The effect of microwave power level

Water layer in case of full load with thickness as 50 mm is chosen for discussion the effect of microwave power level on heating process. Fig. 7 shows the distribution of electric field inside a rectangular waveguide. The vertical axis represents the intensity of the electric field E_y , which is normalized to the amplitude of the input electromagnetic wave $E_{y_{in}}$. It shows a stronger standing wave with a larger amplitude forms in the cavity forward to the water layer while the electric field within the water layer is extinguished. Since the incident wave passing through the cavity having low permittivity is directly irradiated with the water layer having high permittivity, major part of incident wave is reflected and resonated while other part that is minor part is transmitted. Since high power level can penetrate through the surface far over than the low power that

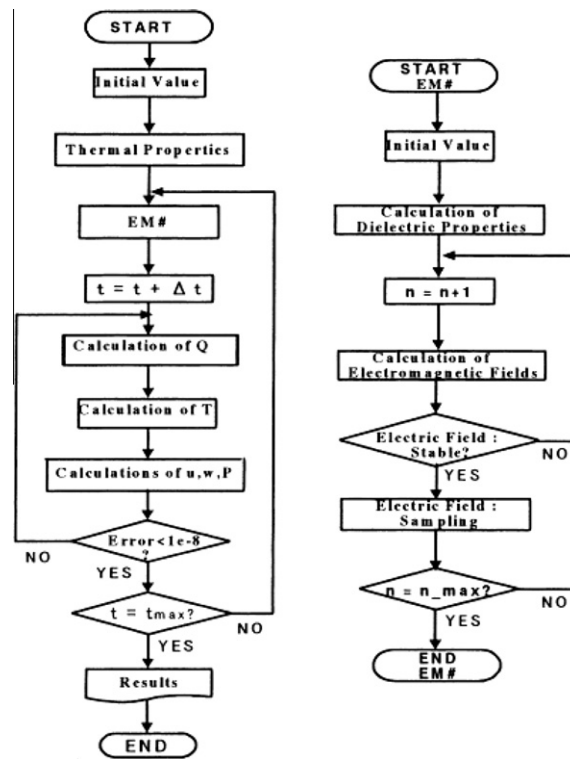


Fig. 4. Computational schemes (EM#: subroutine for calculation of electromagnetic field; n: calculation loop of electromagnetic field). (Reference from Ratanadecho et al. [10].)

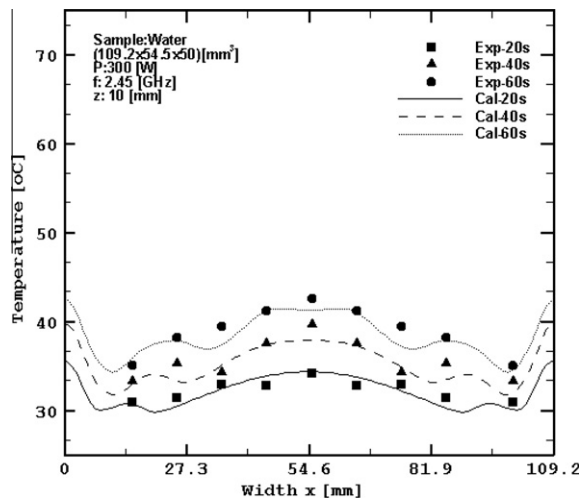


Fig. 5. Distribution of temperature within a water layer as a function of distance at various times.

lead to higher amplitude of transmitted wave within water layer. However, it's quite difficult to see the different from the figure. The effect of microwave power level is dominated in figure of temperature profile and velocity field.

Figs. 8(a) and 8(b) illustrate temperature contour within a water layer on x-z plane at t = 60 s with microwave power levels of 300 W and 1000 W, respectively. The contour of temperature is symmetry between left and right sides. The result shows the highest temperature in the upper region of heating water layer with the temperature decreasing towards the lower wall. In case of high microwave power level (1000 W), temperature is greater near top surface and it is locally high inside the layer. Furthermore, it is evident that the heating rate is higher in this case than lower power (300 W). This is because of the penetration depth heating effect, which increases a larger part of the incident wave can penetrate further into the water layer.

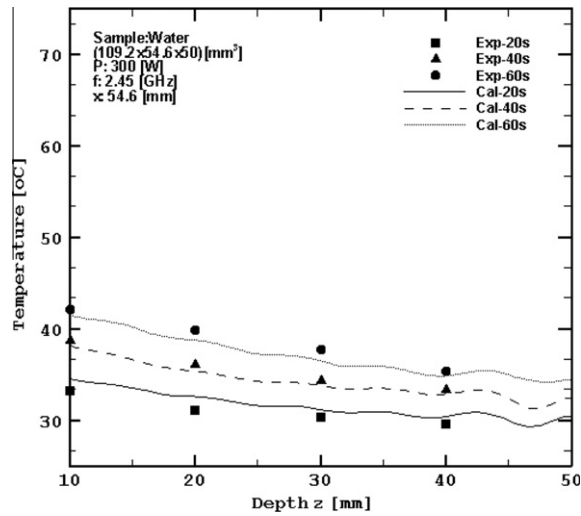


Fig. 6. Distribution of temperature within a water layer as a function of distance at various times.

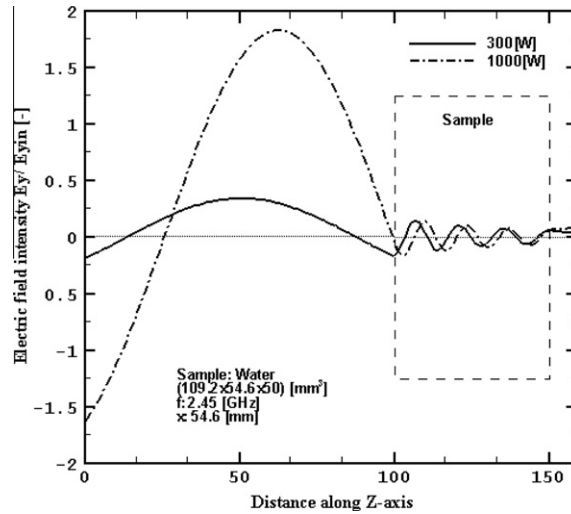


Fig. 7. Distribution of electric field inside a rectangular waveguide at microwave power levels of 300 W and 1000 W.

The velocity fields within the water layer on x - z plane at low and high power level are showed in Figs. 9(a) and 9(b), respectively. These are corresponding to temperature contour in Figs. 8(a) and 8(b). The movement of liquid particles induced by high power was stronger than at low power but the pattern of movement is similar. At the early stage of heating, the effect of conduction plays the greatest role than convection mode. As the heating proceeds, the local heating on the surface water layer causes the difference of surface tension on the surface of water layer, which leads to the convective flow of water (Marangoni flow). This causes water to flow from the hot region (higher power absorbed) at the central region of water layer to the colder region (lower power absorbed) at the side wall of container. In the final stage of heating, the effect of convective flow becomes stronger and plays a more important role, especially at the upper portion of the side walls of container. However, at the bottom region of the walls where the convection plays the smallest, temperature distributions are primarily governed by the conduction mode.

5.3. The effect of placement inside a rectangular waveguide

This section discusses the effect of placement of water layer inside the rectangular waveguide. S0, S10, and S20 are placements of water layer inside the waveguide which are investigated. S represents the placement and the number (0, 10 and 20) mean distance between the center of waveguide, and water layer in mm. The volume ($x \times y \times z$) of the water layer is

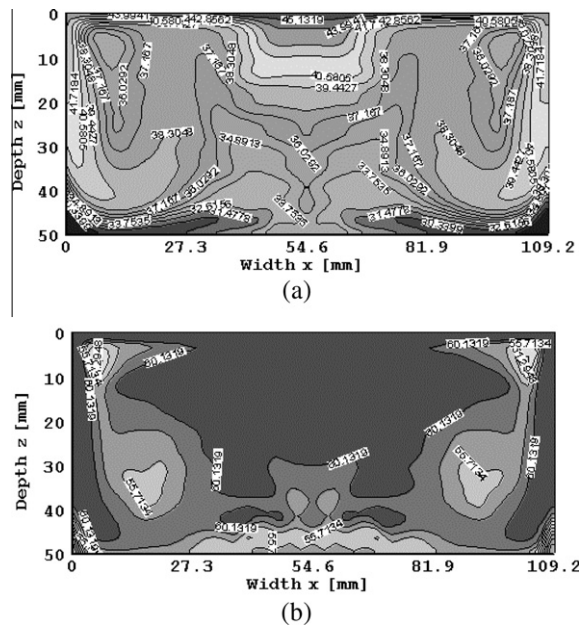


Fig. 8. Temperature contour within water layer at $t = 60$ s; (a) $P = 300$ W; (b) $P = 1000$ W.

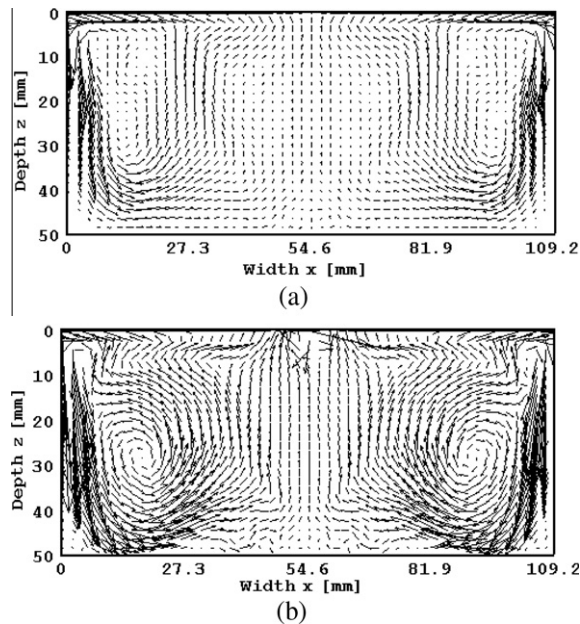


Fig. 9. Flow field within water layer at $t = 60$ s; (a) $P = 300$ W; (b) $P = 1000$ W.

$54.6 \times 54.6 \times 50 \text{ mm}^3$. The microwave power level is 300 W, operating at a frequency of 2.45 GHz. The investigated phenomena are shown in Figs. 10–12.

Fig. 10 presents the distribution of electric field inside the waveguide. It shows considerably uniform distribution of electric field when the sample is located at the center (S0), whereas distribution of electric field is relatively not uniform when location of the sample is shifted to 10 and 20 mm away from the center, respectively denoted by S10 and S20.

The temperature contours within the water layer with various placements inside the guide are shown in Figs. 11(a)–11(c). The distribution of temperature when the sample is located at the center (S0) is symmetry and is similar with the case of full load. In the upper region of heating is high temperature and decreasing towards the lower wall. However, at the side wall has temperature greater than the center of water layer. Figs. 11(b) and 11(c) are distribution of temperature when

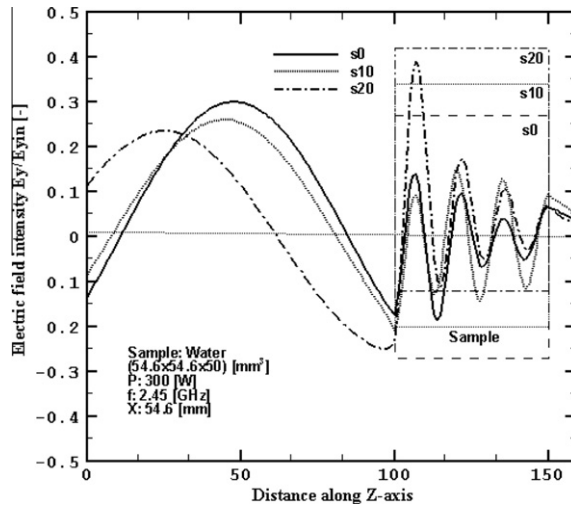


Fig. 10. Distribution of electric field inside a rectangular waveguide with various placements of water layer.

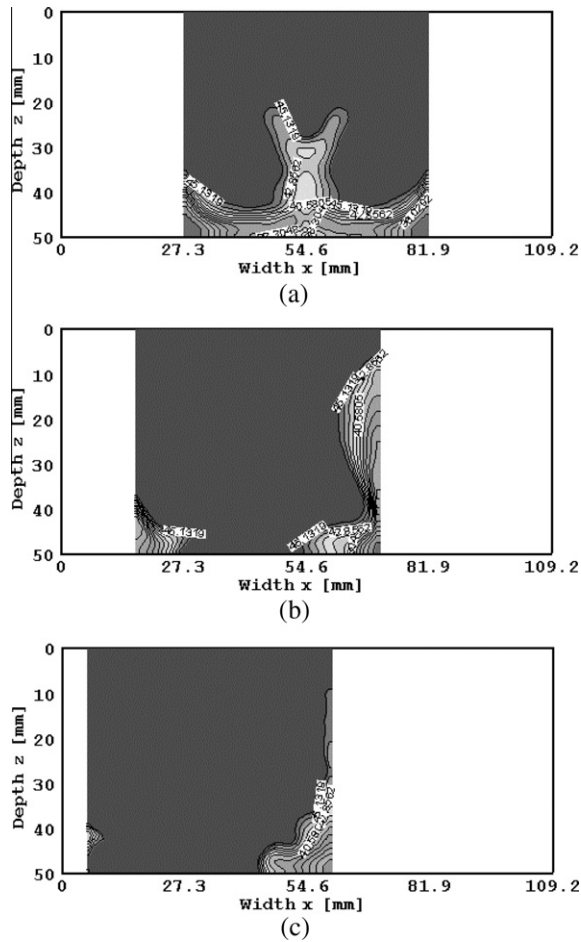


Fig. 11. Temperature contour within water layer with various placements inside the waveguide ($P = 300 \text{ W}$, $t = 60 \text{ s}$); (a) S0, (b) S10 and (c) S20.

placement of the sample is shifted to 10 and 20 mm away from the center, respectively (S10 and S20). Temperature contour is asymmetry between left and right sides. Temperature distribute from the corner of sample and toward the lower. Since the

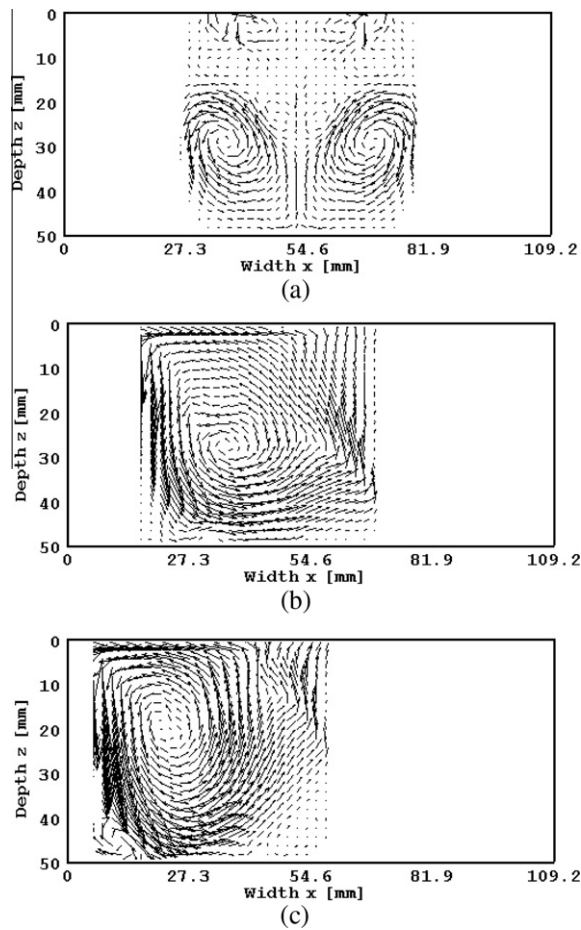


Fig. 12. Flow field within water layer at various placements inside the waveguide ($P = 300 \text{ W}$, $t = 60 \text{ s}$); (a) S0, (b) S10 and (c) S20

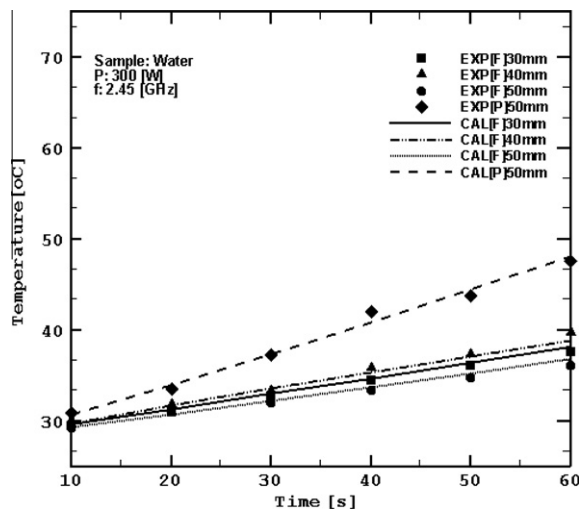


Fig. 13. Temperature profile within water layer with various volumes in 60 s.

originality of heating is changing from center of sample to the position is displaced from center of sample by 10 and 20 mm, respectively. In additionally, the water layer when location of the sample is shifted to 20 mm away from the center has

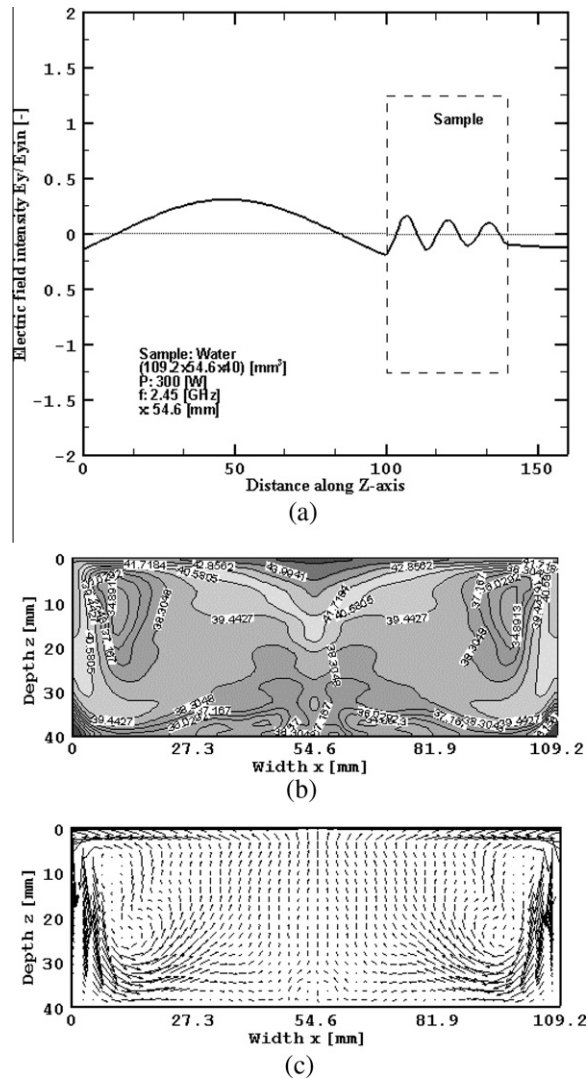


Fig. 14. Heating phenomena in case of full load with thickness as 40 mm ($P = 300$ W, $t = 60$ s); (a) electric field inside the waveguide; (b, c) heat and flow within water layer.

changing rate of temperature higher than the other locations. Since sample has its length smaller than the waveguide width, waves reflect disorderly corresponding to a multimode of field pattern. The temperature profiles are corresponding to distribution of electric field.

Velocity field within water layer on x - z plane are illustrated in Figs. 12(a)–12(c). Several circulations are observed in Fig. 12(a). When location of the sample is shifted to 10 and 20 mm away from the center as respectively shown in Figs. 12(b) and 12(c), there appears the transition from several circulations to one larger circulation. The vectors are rigorous near the upper left corner. The velocity fields have a trend corresponding to that of temperature profile.

5.4. The effect of sample volume

For this section, the effect of sample volume is explained in details. Full load with various thicknesses (30, 40 and 50 mm) and partial load with thickness of 50 mm are studied. Microwave power level of 300 W is considered. Fig. 13 presents the temperature of water layer in 60 s with various volumes. From figure, partial load with thickness as 50 mm has the highest temperature because it has a small volume so rate change of temperature due to heat generation rate per unit volume is higher than large volume. However, the exception is observed in case of full load with thickness as 40 mm. It is found higher temperature than case of full load with thickness as 30 mm. The reason of this result is the penetration depth of microwave within water layer. By the way, the penetration depth close to its thickness that results in the interference of waves reflected from the interface of water and air at the lower side due to the difference of dielectric properties of water and

air. Consequently, the reflection and transmission components at each interface contribute to the resonance of standing wave inside the water sample. Therefore the field distribution does not possess an exponential decay from the surface. Fig. 14 shows heating phenomena in case of full load with thickness as 40 mm. The results are similar with case of full load with thickness of 50 mm.

6. Conclusion

The numerical analysis in this paper describes many of the important interactions that arise during microwave heating of water layer by using a rectangular waveguide. The following summarizes the conclusions of this work:

- A mathematical model of microwave heating by using rectangular waveguide is presented which is in relatively good agreement with the results of the experiment. The model used successfully describes the heating phenomena of water layer under various conditions.
- The temperature profiles and velocity fields within water layer are governed by the electric field as well as dielectric properties of water.
- The distribution of heating position primarily depends on the penetration depth of microwave within water layer.
- The volume of water layer has an effect on phenomena of microwave heating. Small volume and thickness close to penetration depth of water layer has greater distribution of temperature due to larger heat generation rate per unit volume and the reflection and transmission components at each interface contribute to a stronger resonance of standing wave within the sample.
- The placement of water layer inside a waveguide is proved to have an important effect on uniformity of distribution. When the water layer is placed off center, it reveals asymmetry heating and flow patterns.
- Natural convection due to buoyancy force strongly affects on flow pattern within water layer during microwave heating process.

The next steps of the research in this problem will be to investigate more associated parameters and develop the three-dimensional mathematical model.

Acknowledgements

The authors gratefully acknowledge the financial support provided by the Thailand Research Fund and the National Research University Project of Thailand Office of Higher Education Commission for the simulation facilities described in this paper.

References

- [1] A.K. Datta, H. Prosetya, W. Hu, Mathematical modeling of batch heating of liquids in a microwave cavity, *J. Microw. Power Electromagn. Energy* 27 (1992) 38–48.
- [2] X. Jia, M. Bialkowski, Simulation of microwave field and power distribution in a cavity by a three dimension finite element method, *J. Microw. Power Electromagn. Energy* 27 (1) (1992) 11–22.
- [3] F. Liu, I. Turner, M. Bialowski, A finite-difference time-domain simulation of power density distribution in a dielectric loaded microwave cavity, *J. Microw. Power Electromagn. Energy* 29 (3) (1994) 138–147.
- [4] D.C. Dibben, A.C. Metaxas, Frequency domain vs. time domain finite element methods for calculation of fields in multimode cavities, *IEEE Trans. Magn.* 33 (2) (1997) 1468–1471.
- [5] S. Tada, R. Echigo, H. Yoshida, Numerical analysis of electromagnetic wave in a partially loaded microwave applicator, *Int. J. Heat Mass Transfer* 41 (1997) 709–718.
- [6] Q. Zhang, T.H. Jackson, A. Ungan, Numerical modeling of microwave induced natural convection, *Int. J. Heat Mass Transfer* 43 (8) (2000) 2141–2154.
- [7] K.G. Ayappa, S. Brandon, et al, Microwave driven convection in a square cavity, *AIChE J.* 31 (5) (1985) 842–848.
- [8] S. Chatterjee, T. Basak, S.K. Das, Microwave driven convection in a rotating cylindrical cavity: a numerical study, *J. Food Eng.* 79 (2007) 1269–1279.
- [9] J. Zhu, A.V. Kuznetsov, K.P. Sandeep, Mathematical modeling of continuous flow microwave heating of liquid (effect of dielectric properties and design parameters), *Int. J. Therm. Sci.* 46 (2007) 328–341.
- [10] P. Rattanadecho, K. Aoki, M. Akahori, A numerical and experimental investigation of the modeling of microwave heating for liquid layers using a rectangular waveguide (effects of natural convection and dielectric properties), *Appl. Math. Model.* 26 (2000) 449–472.
- [11] T. Basak, Role of resonance on microwave heating of oil-water emulsions, *AIChE J.* 50 (2004) 2659–2675.
- [12] P. Rattanadecho, K. Aoki, M. Akahori, Influence of irradiation time, particle sizes and initial moisture content during microwave drying of multi-layered capillary porous materials, *ASME J. Heat Transfer* 124 (1) (2002) 151–161.
- [13] P. Rattanadecho, K. Aoki, M. Akahori, The characteristics of microwave melting of frozen packed bed using a rectangular waveguide, *IEEE Trans. Microw. Theor. Tech.* 50 (6) (2002) 1495–1502.
- [14] P. Rattanadecho, N. Suwannapum, W. Cha-um, Interactions between electromagnetic and thermal fields in microwave heating of hardened type I-cement paste using a rectangular waveguide (influence of frequency and sample size), *ASME J. Heat Transfer* 131 (2009) 082101–082112.
- [15] W. Cha-um, P. Rattanadecho, W. Pakdee, Experimental analysis of microwave heating of dielectric materials using a rectangular wave guide (MODE: TE₁₀) (case study: water layer and saturated porous medium), *Exp. Therm. Fluid Sci.* 33 (2009) 472–481.
- [16] W. Cha-um, P. Rattanadecho, W. Pakdee, Experimental and numerical analysis of microwave heating of water and oil using a rectangular wave guide: influence of sample sizes, positions, and microwave power, *Food Bioprocess Technol.* 4 (4) (2011) 44–558.
- [17] W. Klinbun, P. Rattanadecho, W. Pakdee, Microwave heating of saturated packed bed using a rectangular waveguide (TE₁₀ mode): influence of particle size, sample dimension, frequency, and placement inside the guide, *Int. J. Heat Mass Transfer* 54 (2011) 1763–1774.

- [18] S.V. Patankar, *Numerical Heat Transfer and Fluid Flow*, Hemisphere, New York, 1980.
- [19] K.S. Yee, Numerical solution of initial boundary value problems involving Maxwell's equation in isotropic media, *IEEE Trans. Antenn. Propag.* AP-14 (1966) 302–307.
- [20] G. Mur, Absorbing boundary conditions for the finite-difference approximation of the time-domain electromagnetic-field equations, *IEEE Trans. Electromag. Compat.* EMC-23 (4) (1981) 377–382.